# Enhancing blood glucose control through the fixed point theorem

Ayoub Sakkoum✉, Hamza Toufga, Lahbib Benahmadi🆔, Wafae Chahid🆔 and Mustapha Lhous🆔

*Mathematical Analysis, Algebra and Applications Laboratory,*
*Department of Mathematics and Computer Science, Faculty of Sciences Ain Chock,*
*Hassan II University of Casablanca, B.P. 5366 Maarif Casablanca, Morocco*

**Abstract.** Diabetes is a chronic condition that poses significant health risks globally, arising from the body's inability to effectively utilize insulin produced by the pancreas or insufficient insulin production. This paper proposes a novel approach to diabetes management by focusing on optimal control strategies aimed at regulating blood glucose levels to achieve desired targets. We integrate concepts of output controllability into a discrete-time model that captures the dynamics of glucose and insulin interactions. Applying fixed-point theorems, we define permissible control mechanisms for dealing with the challenge of keeping glucose concentrations within optimal ranges. The theoretical framework is supported by numerical simulations that demonstrate the efficacy of the suggested optimal control method in minimizing blood glucose fluctuations. Our findings shed light on the development of advanced blood glucose control systems, eventually leading to enhanced diabetes management and improved quality of life for individuals impacted by the disease.

## 1 Introduction

Worldwide, 451 million people were affected by diabetes in 2017, and scientists project that the number of individuals with the disease will increase significantly, reaching 643 million by 2030 and 783 million by 2045 [29]. In adults, diabetes and impaired glucose tolerance have been on the rise globally over the last several decades, according to [16]. Type 1, type 2, and gestational diabetes are the three main types of this disease. Type 1 diabetes occurs when the pancreatic insulin-producing cells are destroyed by the immune system.

However, insulin resistance and inactivity are major risk factors for type 2 diabetes. A higher risk of developing type 2 diabetes is associated with gestational diabetes, which arises during pregnancy. Early diagnosis and proper treatment for all types of diabetes, as well as prevention measures for type 2 diabetes, are all helping reduce the diabetes epidemic. To prevent complications like heart disease, kidney issues, renal problems, and nerve damage, diabetes management involves medication, lifestyle modifications, and routine monitoring [17]. When the $\beta$ cells of the Langerhans islets do not work properly, it prevents the body from producing enough insulin, leading to type 1 diabetes. If insulin is not able to reach the cells of the body, type 2 diabetes will develop. according to [18].

The measurements of blood glucose are indicated in millimoles per liter (mmol/L) or milligrams per deciliter (mg/dL). The pancreas regulates blood glucose levels in the human body by producing and releasing the hormones insulin and glucagon, thereby adjusting the physiological range of 70–120 mg/dl. The normal blood glucose levels in humans are determined by the amount of glucose in the blood. Individuals without diabetes typically have fasting blood glucose levels ranging from 3.9 to 5.5 mmol/L (70–100 mg/dL) and less than 7.8 mmol/L (140 mg/dL) two hours after a meal. The typical range for kids and young adults is 3.3 to 5.5 mmol/L (60 to 100 mg/dL) for those under 12 years of age and 3.9 to 5.5 mmol/L (70 to 100 mg/dL) for those older than 12. For infants, the levels range from 2.2 to 5.5 mmol/L for those under 24 hours and 2.8 to 5.5 mmol/L for those over 24 hours old [8,9,14,15,28,34]. According to the American Diabetes Association (ADA), fasting blood glucose levels less than 100 mg/dl indicate poor glucose tolerance, while readings greater than 126 mg/dl may indicate diabetes. Individual variations in normal blood glucose levels should be considered for tailored advice [7]. The discovery of insulin and its importance in diabetes was such a significant medical achievement that a number of scientists, such as Oskar Minkowski and Joseph von Mering, were awarded the Nobel Prize [27]. Diabetes research seeks to advance diagnosis, therapy, and possibly even a cure.The discovery of insulin in the 1920s completely changed the treatment of diabetes. Recent studies have found genetic variations linked to the development of diabetes. Current treatments use insulin therapy and other alternatives to manage blood glucose levels and prevent challenges [24].

For diabetic patients, mathematical modeling is essential for controlling blood glucose levels. This modeling can take many forms, from simple linearization techniques to complex physiological-based models that consider insulin production, action, and glucose dynamics. In recent years, there has been an increase in the number of individuals with type 2 diabetes. Over the past 50 years, compartmental models have been used to characterize the glucose-insulin system, ranging from simple models like Bergman's [12] to more complex ones like Hovorka [23], UVa-Padova [30] and Sorensen's [18]. Several researchers have developed a mathematical model of the human glucose-insulin system in order to effectively manage blood glucose levels. Mathematical modeling seeks to forecast changes in blood glucose levels as a result of several factors outside the body. Bergman et al. [11,12] came up with a simple compartmental model

of nonlinear ordinary differential equations that shows how different types of blood glucose are connected to the hormone insulin. Blood glucose, insulin, and a hormone were considered to be in two different compartments and to interact with each other. Subashri et al. [6] applied state-space analysis and machine learning approaches on dynamic simulations of glucose-insulin interaction to manage blood glucose levels in diabetic individuals. Ankit Sharma et al. [33] analyze several mathematical models and control methods for diabetes management, including genetic algorithms, neural networks, sliding mode controllers, and modeling predictive controllers. Ali Cinar et al. [17] look at a number of modeling approaches for studying how glucose and insulin levels change in the body, showing how important compartmental models are. Pappada et al. [31] developed a neural network model to predict blood glucose levels. Bergman and colleagues [10,12] used nonlinear ordinary differential equations to examine the relationship between different types of blood glucose and insulin hormones. Storis and colleagues [35] suggested a discretized model for glucose breakdown and reactions with six states. Adoum et al. [1, 2] investigated mathematical models of insulin and glucose systems in Chadians with type 2 diabetes.

In recent years, a number of studies have been conducted on controllability in linear and non-linear dynamical systems, including complete, small, local, regional, near, null, and output controllability. In the first paper by Dimplekumar N. Chalishajar et al. [13], they look at how to control the trajectory of an abstract nonlinear integro-differential system in both finite and infinite dimensional space. In the second paper by Lin Tie and Kai-Yuan Cai [37], they look at how to almost control upper-triangular bilinear systems that are not controllable. Lhous et al. [25] described a way to check if the output of nonlinear, infinite-dimensional discrete systems can be controlled. A mathematical model with optimal control was analyzed in [9] to study the epidemic's output toward a desirable disease output. For people with type 1 diabetes, Saleem et al. [21] suggested using linear control for a glucose-insulin-glucagon pump that is made up of several parts. In order to determine whether glucose drives pulsatile insulin secretion or if an intrapancreatic pacemaker passively entrains glucose, Jeppe Sturi et al. [36] investigated whether oscillatory glucose infusion might change the insulin secretion pulse frequency in normal males. Sturis et al. [26] published research that contributed to the discussion and efforts to manage diabetes. Muhammad Farman et al. [19] present a mathematical model of cells, insulin, glucose, and growth hormone that includes the fractional operator. In [20], Muhammad Farman and colleagues discovered a major class of control issues regulated by nonlinear fractal order systems with input and output signals. The aim of the study was to develop a direct transcription method that incorporates impulsive immediate orders. Khalid I.A. Ahmed et al. produced two major papers in [4] and [3] by providing new strategies for diabetes through mathematical modeling, focused on modified minimal models. Another diabetic treatment technique is to use fractal-fractional derivatives in the Atangana-Baleanu model. Mansoor H. Alshehri et al. [5] offered a dynamical analysis of fractional-order IVGTT glucose-insulin interaction, while Sayed Saber [32] also contributed. Please send us the stability analysis and numerical simulations of IVGTT glucose-insulin interaction models with two time delays.

The following is the structure of the remaining sections of this study: Section 2 describes the structure of a discrete-time model with three basic compartments to illustrate the dynamics of glucose and insulin levels over time. We also propose an optimal control problem. In Section 3, we introduce the fixed point method to characterize all admissible controls and select the one with the minimum norm. Section 4 discusses numerical simulations and comparisons of our work with others to demonstrate the model's operation. Section 5 concludes and summarizes the important results of this investigation.

## 2 The mathematical model

### 2.1 The structure of the main model

The glucose-insulin regulation system consists of three basic components: cell membrane permeability to glucose molecules is increased by insulin, the primary regulator of glucose uptake in target cells, $\beta$-cells store and generate insulin in the pancreas and glucose, which is detected by $\beta$-cells as an energy source, releases stored insulin molecules and produces new insulin when blood glucose concentration increases. The abdominal organ, known as the pancreas, is responsible for producing insulin [22]. Insulin plays an important function in ensuring that glucose derived from nutrients in food is properly used or kept in the body. Glucose levels continue to rise after eating because there is insufficient insulin to transfer glucose into cells in the human body. The pancreas stops producing insulin, which leads to type 1 diabetes. Type 2 diabetes develops when the pancreas fails to produce enough insulin. We are specifically focusing on type 1 diabetes. The intestine produces blood glucose from food. Two different compartments contain the blood glucose and the hormone insulin, which interact with each other. The liver can convert blood glucose into glycogen, which tissue metabolism can use with or without insulin's assistance. Under the stimulation of blood glucose, the endocrine system secretes plasma insulin, which then enters a "remote compartment" to accelerate glucose utilization. Insulin metabolism consumes it. Under this assumption. In considering these assumptions and ideas, we present a discrete-time model that represents the dynamics of blood glucose levels and their connection to insulin. The model equations for glucose dynamics are presented below:

$$
\begin{aligned}
g_{i+1} &= (1-a)g_i - h_i g_i + f_i, \\
h_{i+1} &= (1-b)h_i + ck_i, \quad k_{i+1} = (1-d)k_i + u_i,
\end{aligned}
$$

where $g_0 > 0$, $h_0 > 0$, and $k_0 > 0$ are the initial states. The total population is $N_i = g_i + h_i + k_i$.

The blood glucose concentration $g_i$, plasma insulin concentration $h_i$, and insulin's indirect effect on glucose $k_i$ are the variables represented in the equations provided above. The rate constants used in the model are defined according to their biological meaning in Table 1. The stage $f_i$ marks the entry of glucose into the bloodstream, where it splits into two categories: basic external glucose and glucose disorder. The objective is to keep the blood sugar level normal.

**Table 1.** Descriptions of parameters.

| Parameter | Description |
|---|---|
| $f_i$ | The entry rates of exogenous glucose. |
| $u_i$ | The entry rates of insulin released by the endocrine. |
| $a$ | Glucose utilization rate constant$(/min)$. |
| $b$ | Insulin effect rate constant$(/min)$. |
| $c$ | Insulin effect rate constant$(/(pmol/l)/min^2)$. |
| $d$ | Insulin metabolism constant$(/min)$. |

$u_i \in [0,1]$ is the control variable, which is the quantity of insulin produced by the endocrine system or injected indirectly. We generate an output equation to monitor and regulate the glucose levels $y_i = g_i$, $i \in \{0, \dots, N\}$.

## 2.2 The structure of the new model

We adapt our system to a new one, investigate its output controllability, and study optimal control to understand how to apply the fixed point concept. Let us consider the state $\zeta_i = (g_i, h_i, k_i)$, assuming the next system

$$(E) \begin{cases} \zeta_{i+1} &= A_1\zeta_i + A_{2,i}\zeta_i + A_3 u_i, \\ \zeta_0 &\in \mathbb{R}^3, \end{cases}$$

with the corresponding output $y_i = A_4\zeta_i$, $i \in \{0, \dots, N\}$, where $A_1$, $A_2$ and $A_4$ are matrices defined by

$$A_1 = \begin{pmatrix} 1-a & 0 & 0 \\ 0 & 1-b & c \\ 0 & 0 & 1-d \end{pmatrix}, \quad A_3 = \begin{pmatrix} 0 \\ 0 \\ 1 \end{pmatrix}, A_4 = [1,0,0].$$

The variance and nonlinear operator is $A_{2,i}$

$$A_{2,i}: \quad \mathbb{R}^3 \quad \longrightarrow \quad \mathbb{R}^3,$$
$$\begin{pmatrix} x \\ y \\ z \end{pmatrix} \quad \longrightarrow \quad \begin{pmatrix} -yx + f_i \\ 0 \\ 0 \end{pmatrix}.$$

A desired output $y^d = (y_1^d, \dots, y_N^d)$ is proposed, the following path in an attempt to make the blood glucose correspond to the previously imposed output control, which is determined in the natural state at 6 mmol/l. The goal is to find the optimal control $u = (u_0, u_1, \dots, u_{N-1})$ that aligns with the control while minimizing functional cost

$$J(u) = \|u\|^2, \quad \forall \ i \in \{1, \dots, N\},$$

$u_i$ satisfies $y_i = y_i^d$, . We use the state space modeling technique to show how we can represent the input retrieval problem as an optimal control problem with constraints on the final state. For a finite subset $\omega_\varepsilon^n = \{\varepsilon, \varepsilon + 1, \dots, n\}$ of $\mathbb{Z}$,

with $n \geq \varepsilon$, let $l^2(\omega_\varepsilon^n, \mathbb{R}^3)$ be the space in all processes $(t_i)_{i \in \omega_\varepsilon^n}$ , $t_i \in \mathbb{R}^3$. Let $T_1$ and $T_2$ be the operators given by

$$
\begin{array}{rcl}
T_1: & l^2(\omega_{-N}^{-1}; \mathbb{R}^3) & \longrightarrow & l^2(\omega_{-N}^{-1}; \mathbb{R}^3), \\
& (t_{-N}, \ldots, t_{-1}) & \longmapsto & (t_{-N+1}, \ldots, t_{-1}, 0), \\
\\
T_2: & \mathbb{R}^3 & \longrightarrow & l^2(\omega_{-N}^{-1}; \mathbb{R}^3), \\
& p & \longmapsto & (0, \ldots, 0, p)
\end{array}
$$

and $t^i \in l^2(\omega_{-N}^{-1}; \mathbb{R}^2)$ by

$$
\begin{aligned}
t^i &= (t_{-N}^i, \ldots, t_{-1}^i), \\
t_k^i &= \begin{cases} \chi_{i+j} &, \quad \text{if } i+j \geq 0, \\ \chi_0 &, \quad \text{else.} \end{cases}
\end{aligned}
$$

The state of $(\chi_i)_i$ is a solution of the model $(E)$. The order of $(t^i)_i$ is a unique answer to the following equation:

$$
\begin{cases}
t^{i+1} &= T_1 t^i + T_2 \chi_i , \quad i \in \omega_0^{N-1}, \\
t^0 &= (\chi_0, \chi_0, \ldots, \chi_0).
\end{cases}
$$

Let $\varrho_i \in \mathbb{R}^3 \times l^2(\omega_{-N}^{-1}; \mathbb{R}^3)$ be the signals that are described by $\varrho_i = \begin{pmatrix} \chi_i \\ t^i \end{pmatrix}$. The following conclusion follows obviously: [25].

**Proposition 1.** *$(\varrho_i)_{i \in \omega_0^N}$ is the only solution to the difference equation stated by*

$$
(E_1) \begin{cases}
\varrho_{i+1} &= \varphi \varrho_i + \psi_i \varrho_i + \bar{\Theta} u_i , \quad i \in \omega_0^{N-1}, \\
\varrho_0 &= \begin{pmatrix} \chi_0 \\ (\chi_0, \ldots, \chi_0) \end{pmatrix},
\end{cases}
$$

*where* $\varphi = \begin{pmatrix} A_1 & 0 \\ T_2 & T_1 \end{pmatrix}$, $\psi_i = \begin{pmatrix} A_{2,i} & 0 \\ 0 & 0 \end{pmatrix}$ *and* $\bar{\Theta} = \begin{pmatrix} A_3 \\ 0 \end{pmatrix}$.

*Remark 1.* The equality

$$
\varrho_N = \begin{pmatrix} \chi_N \\ t^N \end{pmatrix} = \begin{pmatrix} \chi_N \\ (\chi_0, \ldots, \chi_{N-1}) \end{pmatrix}
$$

enables us to integrate the system $(E)$ trajectory $(\chi_0, \chi_1, \ldots, \chi_N)$ to the final state $\varrho_N$ of our system $(E_1)$. This means that the input retrieval problem is comparable to an optimal control problem with restrictions on the $\varrho_N$ final state.

## 2.3   The optimal control problem

Consider the operator $\tau$, defined as

$$
\begin{array}{rcl}
\tau: & \mathbb{R}^3 \times l^2(\omega_{-N}^{-1}; \mathbb{R}^3) & \longrightarrow & l^2(\omega_1^N; \mathbb{R}), \\
& (x, (\zeta_i)_{-N \leq i \leq 0}) & \longmapsto & (l_1, \ldots, l_N)
\end{array} \tag{2.1}
$$

with $l_i = A_4\zeta_{i-N}$, for all i $\in \omega_1^{N-1}$   and   $l_N = A_4x$.

To solve this control problem, the Definitions 1, 2, and Proposition 2 are firstly used [25].

DEFINITION 1.

**a)** On $\omega_1^N$, the system $(E)$ is supposed to be exactly output controlled if $\forall\chi_0 \in \mathbb{R}^3 \times l^2(\omega_{-N}^{-1};\mathbb{R}^3)$, $\forall y \in l^2(\omega^N;\mathbb{R})$, $\exists u \in l^2(\omega^{N-1};U)$ in order to $A_4\chi_i = y_i$, $i \in \omega_1^N$.

**b)** On $\omega_1^N$, the system $(E)$ is supposed to be weakly output controlled if $\forall\epsilon > 0$, $\forall\chi_0 \in \mathbb{R}^3 \times l^2(\omega_{-N}^{-1};\mathbb{R}^3)$,   $\forall y \in l^2(\omega_1^N;\mathbb{R})$, $\exists u$ such that $\|A_4\chi_i - y\|\mathbb{R} \le \epsilon$.

DEFINITION 2.

**a)** The system $(E)$ is supposed to be $\tau$-controllable on $\omega_1^N$ if $\forall\varrho_0 \in \mathbb{R}^3 \times l^2(\omega_{-N}^{-1};\mathbb{R}^3)$, $\forall y^d \in l^2(\omega_1^N;\mathbb{R})$,   $\exists u \in l^2(\omega_0^{N-1};[0,1])$ in order to $\tau\varrho_N = y^d$.

**b)** The system $(E)$ is supposed to be $\tau$-weakly controllable on $\omega_1^N$ if $\forall\epsilon > 0$,   $\forall\varrho_0 \in \mathbb{R}^3 \times l^2(\omega_{-N}^{-1};\mathbb{R}^3)$,   $\forall y^d \in l^2(\omega_1^N;\mathbb{R})$, $\exists u$ such that $\|\tau\varrho_N - y^d\|l^2(\omega_1^N;\mathbb{R}) \le \epsilon$.

Based on the definition provided, it is easy to determine the following:
($i$) (E) is exactly output controllable $\omega_1^N \Leftrightarrow (E_1)$ is $\tau$-controllable on $\omega_1^N$;
($ii$) (E) is weakly output controllable on $\omega_1^N \Leftrightarrow (E_1)$ is $\tau$-weakly controllable on $\omega_1^N$.

**Proposition 2.** *Assuming a desired output* $y^d = (y_1^d, \ldots, y_N^d) \in l^2(\omega_1^N;\mathbb{R})$, *output controllability defined by*

$$(1) \quad \begin{cases} \text{Find } u_1^* \text{ so that} \\ A_4\chi_i = y_i^d, \quad \forall \ i \in \omega_1^N, & (i) \\ \|u_1^*\| = inf\{ \ \|u_2\| \ / \ u_2 \ verify \ (i)\} & (ii) \end{cases}$$

*and the $\tau$-controllability defined by*

$$(2) \quad \begin{cases} \text{Find } u_1^* \text{ so that} \\ \tau\varrho_N = y^d \in l^2(\omega_1^N;\mathbb{R}^2), & (j) \\ \|u_1^*\| = inf\{ \ \|u_2\| \ / \ u_2 \ verify \ (j)\} & (jj). \end{cases}$$

*are eqivalantent and have the same solution* $u_1^*$.

According to Proposition 2, in order to resolve problems (1) and (2), we have to find a control $u^*$ that ensures $\tau$-controllability of system $(E_1)$ with a low cost. Consider the following discrete system:

$$(E_1) \quad \begin{cases} \varrho_{i+1} &= \varphi\varrho_i + \ \psi_i\varrho_i + \bar{\Theta}u_i \ , \ i \in \omega_0^{N-1}, \\ \varrho_0 & \text{is given}, \end{cases}$$

where $\varrho_i \in \mathcal{X} = \mathbb{R}^3 \times l^2(\omega_{-N}^{-1}; \mathbb{R}^3)$ represents the system's state $(E_1)$, and $u_i \in U = [0,1]$ represents the control variable, $\varphi \in \mathcal{L}(\mathcal{X})$ and $\bar{\Theta} \in \mathcal{L}(U, \mathbb{R}^3)$. Given the following control problem: Assume a desired trajectory $y^d = (y_1^d, \dots, y_N^d)$, then identify the control $u^*$ that optimizes the functional of expense

$$J(u) = \|u\|^2.$$

Regarding all controls satisfying $\tau \varrho_N = y^d$, $\varrho_N$ is the final state of system $(E_1)$ at instant $N$, and $\tau$ is given by (2.1). The desired control is denoted as $u^*$, and the solution for the system $(E_1)$ is

$$\varrho_i = \varphi^i \varrho_0 + \sum_{j=0}^{i-1} \varphi^j \psi_{i-1-j} \varrho_{i-1-j} + \sum_{j=0}^{i-1} \varphi^j \bar{\Theta} u_{i-1-j}, \quad i \in \omega_1^N. \tag{2.2}$$

Consider a linear operator $L$ defined on $\mathcal{T} = l^2(\omega_1^N; \mathcal{X})$ by

$$L: \quad \mathcal{T} = l^2(\omega_1^N; \mathcal{X}) \quad \longrightarrow \quad \mathcal{T},$$
$$\xi = (\xi_1, \dots, \xi_N) \quad \longmapsto \quad L\xi = (L\xi)_{1 \le i \le N},$$

where

$$\begin{cases} (L\xi)_i &= \varphi^{i-1}\psi \varrho_0 + \displaystyle\sum_{j=0}^{i-2} \varphi^j \psi_{i-1-j}\xi_{i-1-j}; \quad 2 \le i \le N, \\ (L\xi)_1 &= \psi \varrho_0. \end{cases}$$

Given $\xi = (\xi_i)_{i \in \omega_1^N} \in \mathcal{T}$ with $\xi_i = \left(x_i, y_i, z_i, (v_1^i, \dots, v_N^i)\right)^T \in \mathcal{X}$, then

$$(L\xi)_1 = \left( \begin{pmatrix} -x_0 y_0 + f_0 \\ 0 \\ 0 \\ (0, \dots, 0) \end{pmatrix} \right),$$

and let's denote

$$A1 = \begin{pmatrix} (1-a)(-x_0 y_0 + f_0) \\ 0 \\ 0 \end{pmatrix}, \quad A2 = \begin{pmatrix} (1-a)^{i-2}(-x_0 y_0 + f_0) \\ 0 \\ 0 \end{pmatrix}$$

then

$$(L\xi)_i = \left( \begin{pmatrix} (1-a)^{i-1}(-x_0 y_0 + f_0) \\ 0 \\ 0 \end{pmatrix} \atop \left( \underbrace{0, \dots, 0}_{N-i+1}, \begin{pmatrix} -x_0 y_0 + f_0 \\ 0 \\ 0 \end{pmatrix}, A1, \dots, A2 \right) \right)$$

$$+$$

$$
\left(
\begin{pmatrix}
\sum_{j=0}^{i-2}(1-a)^j(-x_{i-1-j}y_{i-1-j}+f_{i-1-j}) \\
0 \\
0
\end{pmatrix}
\right.
$$

$$
\left(\underbrace{0,\ldots,0,}_{N-i+2}
\begin{pmatrix}
-x_1y_1+f_1 \\
0 \\
0
\end{pmatrix},
\begin{pmatrix}
-x_2y_2+f_2+(1-a)(-x_1y_1+f_1) \\
0 \\
0
\end{pmatrix},\ldots,
\right.
$$

$$
\left.\left.
\begin{pmatrix}
\sum_{j=1}^{i-2}(1-a)^{j-1}(-x_{i-1-j}y_{i-1-j}+f_{i-1-j}) \\
0 \\
0
\end{pmatrix}
\right)\right),
$$

$i \in \omega_1^N$. Consider the linear operator $H$ defined on $\mathcal{U}$ by

$$
\begin{aligned}
H: \quad \mathcal{U} = l^2(\omega_0^{N-1};[0,1]) &\longrightarrow \mathcal{T}, \\
u = (u_0,\ldots,u_{N-1}) &\longmapsto Hu,
\end{aligned}
$$

where

$$
(Hu)_i = \sum_{j=0}^{i-1}\varphi^j\bar{\Theta}u_{i-1-j}, \quad i \in \omega_1^N.
$$

We have $\forall i \in \omega_1^N$ :

$$
(Hu)_i =
$$

$$
\left(
\begin{pmatrix}
0 \\
c\sum_{j=1}^{i-1}\left(\sum_{k=0}^{j-1}(1-b)^{j-1-k}(1-d)^k\right)u_{i-1-j} \\
\sum_{j=1}^{i-1}(1-d)^j u_{i-1-j}
\end{pmatrix}
\right.
$$

$$
\left(\underbrace{0,\ldots,0,}_{N-i+1}
\begin{pmatrix}
0 \\
0 \\
u_0
\end{pmatrix},
\begin{pmatrix}
0 \\
cu_0 \\
(1-d)u_0+u_1
\end{pmatrix},
\begin{pmatrix}
0 \\
c(u_1+\sum_{s=0}^{1}(1-b)^{1-s}(1-d)^s u_0) \\
(1-d)^2 u_0+(1-d)u_1+u_2
\end{pmatrix},
\right.
$$

$$
\left.\left.
\ldots,
\begin{pmatrix}
0 \\
c\left(u_{i-3}+\sum_{j=3}^{i-1}\sum_{s=0}^{j-2}(1-b)^{j-s-2}(1-d)^s\right)u_{i-1-j} \\
\sum_{j=1}^{i-1}(1-d)^{j-1}u_{i-1-j}
\end{pmatrix}
\right)\right)
$$

Thus, we may rewrite the Equation (2.2) as

$$
\varrho = (\varrho_1,\ldots,\varrho_N) = \tilde{\varphi}\varrho_0 + L\varrho + Hu,
$$

where

$$\tilde{\varphi}\varrho_0 = (\varphi^i \varrho_0)_{1 \le i \le N}, \ KerH = \{0\}, \ (KerH)^\top = \mathcal{U} = l^2(\omega_0^{N-1}, \mathbb{R}),$$

$$Range(H) = \left\{ z = (z_i)_{i \in \omega_1^N} \in l^2(\omega_0^{N-1}, \mathcal{X}) / z_i = A3 \right.$$

$$\left. \text{with} \quad i \in \omega_1^N, \ \beta_i \in \mathbb{R}, \ \alpha_1 = 0 \ \text{and} \ \alpha_{i+1} = c\beta_i + (1-b)\alpha_3 \right\},$$

where

$$A3 = \left( \begin{pmatrix} 0 \\ \alpha_i \\ \beta_i \end{pmatrix} \\ \left( \underbrace{0, \dots, 0,}_{N-i+1} \begin{pmatrix} 0 \\ \alpha_1 \\ \beta_1 \end{pmatrix}, \dots, \begin{pmatrix} 0 \\ \alpha_{i-1} \\ \beta_{i-1} \end{pmatrix} \right) \right),$$

Its inverse is defined by

$$\begin{cases} H^{-1} \ : \qquad\qquad Range(H) \qquad\qquad \longrightarrow \ \mathcal{U}, \\ \\ z = \left( \begin{pmatrix} 0 \\ \alpha_i \\ \beta_i \end{pmatrix} \\ \left( \underbrace{0, \dots, 0,}_{N-i+1} \begin{pmatrix} 0 \\ \alpha_1 \\ \beta_1 \end{pmatrix}, \dots, \begin{pmatrix} 0 \\ \alpha_{i-1} \\ \beta_{i-1} \end{pmatrix} \right) \right) \qquad \longrightarrow \ H(z), \end{cases}$$

where $H(z) = u/ \begin{cases} u_0 = \beta_1, \\ u_i = \beta_{i+1} - (1-d)\beta_i, \quad i \in \omega_1^{N-1}. \end{cases}$

We introduce the pseudo inverse operator of $H$

$$H^\dagger : x + y \in Range(H) \bigoplus Range(H)^\perp \to \tilde{H}^{-1}(x) \in \mathcal{U}.$$

The operator $H^\dagger$ is defined on all the space $\mathcal{T}$ because $Range(H)$ is closed and we have

$$\begin{cases} HH^\dagger x &= x, \quad \forall x \in Range(H), \\ H^\dagger H y &= y, \quad \forall y \in \mathcal{U}. \end{cases}$$

## 3 Fixed point method

### 3.1 Description of optimal control

Assume $y^d = (y_1^d, \dots, y_N^d)$ is a predefined output. This section aims to define a set of all acceptable controls by examining the fixed points of a carefully selected function. In particular, we will describe the set $\mathcal{U}_{ad}$, which includes all controls that ensure $\tau$-controllability

$$\mathcal{U}_{ad} = \{ u \in l^2(\omega_0^{N-1}; [0,1]) \ / \ \tau\varrho_N = y^d \},$$

where $(\varrho_0, \dots, \varrho_N)$ is the trajectory which takes system from the initial state $\varrho_0$. Let $p : T \longrightarrow Range(H)$ be any projection on $Range(H)$ and $\bar{\varrho} \neq 0$ be any fixed element

of $Range(H)$, we define

$$f_{\bar{\varrho}}: \quad \mathcal{T} \quad \longrightarrow \quad Range(H),$$
$$\varrho \quad \longmapsto \quad f_{\bar{\varrho}}(\varrho) = \begin{cases} 0, & \text{if and only if } \tau\varrho_N = y^d, \\ \bar{\varrho}, & \text{otherwise} \end{cases}$$

and let

$$\xi: \quad \mathcal{T} \quad \longrightarrow \quad \mathcal{T},$$
$$\varrho \quad \longmapsto \quad \xi(\varrho) = \varrho - \tilde{\varphi}\varrho_0 - L\varrho.$$

Then,

$$(\xi(\varrho))_i = \varrho_i - \left( \begin{pmatrix} (1-a)^i x_0 \\ (1-b)^i y_0 + c\sum_{j=0}^{i-1}(1-b)^{i-1-l}(1-d)^l z_0 \\ (1-d)^i z_0 \end{pmatrix} \right.$$
$$\left( \underbrace{\begin{pmatrix} 0 \\ 0 \\ 0 \end{pmatrix}, \ldots, \begin{pmatrix} 0 \\ 0 \\ 0 \end{pmatrix}}_{N-i}, \begin{pmatrix} x_0 \\ y_0 \\ z_0 \end{pmatrix}, \begin{pmatrix} (1-a)x_0 \\ (1-b)y_0 + cz_0 \\ (1-d)z_0 \end{pmatrix}, \ldots, \right.$$
$$\left. \begin{pmatrix} (1-a)^{i-1} x_0 \\ (1-b)^{i-1} y_0 + c\sum_{j=0}^{i-2}(1-b)^{i-2-l}(1-d)^l z_0 \\ (1-d)^{i-1} z_0 \end{pmatrix} \right) \right)$$
$$- (L\varrho)_i$$

and we analyze the mapping

$$g: \quad \mathcal{T} \quad \longrightarrow \quad \mathcal{T},$$
$$\varrho \quad \longmapsto \quad g(\varrho) = \tilde{\varphi}\varrho_0 + L\varrho + p\xi(\varrho) + f_{\bar{\varrho}}(\varrho).$$

Next, we present the following proposition

**Proposition 3.** *Let $P_g = \{\varrho \in \mathcal{T} \ / \ g(\varrho) = \varrho\}$ represent the set of all fixed points of $g$. Then,*

$$\mathcal{U}_{ad} = \bigcup_{\varrho \in P_g} H^\dagger \xi(\varrho).$$

*Proof.*   Let $\varrho^* \in P_g$, we have

$$g(\varrho^*) = \tilde{\varphi}\varrho_0 + L\varrho^* + p\xi(\varrho^*) + f_{\varrho^*}(\varrho) = \varrho^*, \tag{3.1}$$

then

$$\varrho^* - \tilde{\varphi}\varrho_0 - L\varrho^* = p\xi(\varrho^*) + f_{\bar{\varrho}}(\varrho^*),$$

which implies that

$$\xi(\varrho^*) = p\xi(\varrho^*) + f_{\bar{\varrho}}(\varrho^*) \ \in Range(H),$$

that means $p\xi(\varrho^*) = \xi(\varrho^*)$, and $f_{\bar{\varrho}}(\varrho^*) = 0$ which carries that $\tau\varrho_N^* = y^d$. Thus, the Equation (3.1) becomes

$$\varrho^* = \tilde{\varphi}\varrho_0 + L\varrho^* + \xi(\varrho^*) = \tilde{\varphi}\varrho_0 + L\varrho^* + HH^\dagger \xi(\varrho^*). \tag{3.2}$$

Let $u^* = H^\dagger \xi(\varrho^*)$, with and $\varrho^* \in P_g$, then,

$$Hu^* = HH^\dagger \xi(\varrho^*)$$

and from (3.2), we have

$$Hu^* = HH^\dagger \xi(\varrho^*) = \varrho^* - \tilde{\varphi}\varrho_0^* - L\varrho^*,$$

which implies that

$$\begin{cases} \varrho^* &= \tilde{\varphi}\varrho_0^* + L\varrho^* + Hu^*, \\ \tau \varrho_N^* &= y^d, \end{cases}$$

thus $u^* \in \mathcal{U}_{ad}$. Consequently, $\forall \varrho \in P_g$, we have $H^\dagger \xi(\varrho) \subset \mathcal{U}_{ad}$ and

$$\bigcup_{\varrho \in P_g} H^\dagger \xi(\varrho) \subset \mathcal{U}_{ad}.$$

Finally, we demonstrate that $\mathcal{U}_{ad} \subset \bigcup_{\varrho \in P_g} H^\dagger \xi(\varrho)$. Let $u^* \in \mathcal{U}_{ad}$ and $(\varrho_1^{u^*}, \ldots, \varrho_{N-1}^{u^*})$ the trajectory of system $(E_1)$ corresponding to control $u^*$, then

$$\begin{cases} \varrho^{u^*} &= \tilde{\varphi}\varrho_0 + L\varrho^{u^*} + Hu^*, \\ \tau \varrho_N^{u^*} &= y^d, \end{cases}$$

and

$$\begin{cases} \xi(\varrho^{u^*}) &= Hu^*, \\ \tau \varrho_N^{u^*} &= y^d. \end{cases}$$

Consequently,

$$\begin{cases} \xi(e^{u^*}) &= Hu^* \in Range(H), \\ f_{\bar{\varrho}}(\varrho^{u^*}) &= 0, \end{cases}$$

and

$$\varrho^{u^*} = \tilde{\varphi}\varrho_0 + L\varrho^{u^*} + p\xi(\varrho^{u^*}) + f_{\bar{\varrho}}(\varrho^{u^*}) = g(\varrho^{u^*}).$$

Then, $\varrho^{u^*}$ is a fixed point of the mapping of $g$, therefore

$$\mathcal{U}_{ad} \subset \bigcup_{\varrho \in P_g} H^\dagger \xi(\varrho).$$

$\square$

*Remark 2.* The fixed points of $g$ do not depend on the selection of the projection $p$ or the element $\bar{\varrho}$. To illustrate, let $p_1$ and $p_2$ be two projections onto *Range H*, and let $\bar{\varrho}_1$ and $\bar{\varrho}_2$ be two non-zero elements from *Range H*. Now, consider the applications.

$$\begin{aligned} g_1 : \quad \mathcal{T} &\longrightarrow \mathcal{T}, \\ \varrho &\longrightarrow g_1(\varrho) = \tilde{\varphi}\varrho_0 + L\varrho + p_1\xi(\varrho) + f_{\bar{\varrho}_1}(\varrho), \end{aligned}$$

$$\begin{aligned} g_2 : \quad \mathcal{T} &\longrightarrow \mathcal{T}, \\ \varrho &\longrightarrow g_2(\varrho) = \tilde{\varphi}\varrho_0 + L\varrho + p_2\xi(\varrho) + f_{\bar{\varrho}_2}(\varrho). \end{aligned}$$

Let $\varrho$ be a fixed point of $g_1$. According to the proof of Proposition 3, we have $\tau \varrho_N = y^d$ and $\xi(\varrho) \in Range\ H$, which implies $p_2\xi(\varrho) = \xi(\varrho)$ and $f_{\bar{\varrho}_1}(\varrho) = 0$. Therefore,

$$g_2(\varrho) = \tilde{\varphi}\varrho_0 + L\varrho + \xi(\varrho) = \varrho.$$

The results show that $\varrho$ is a fixed point of $g_2$. Likewise, by symmetry, it is clear that the fixed points of $g_2$ are also fixed points of $g_1$.

## 3.2    Minimization problem

Based on the proposition above, we may define the set of admissible controls as $\mathcal{U}_{ad}$. We can then choose the controls that have the minimum norm, therefore resolving the next problem

$$\bar{\mathcal{P}} : \min_{u \in \mathcal{U}_{ad}} (J(u) = \|u\|^2),$$

then,

$$\mathcal{U}_{ad} = \bigcup_{\varrho \in P_g} H^\dagger \xi(\varrho),$$

while $P_g$ the set of all fixed point of g, and $\mathcal{U}_{ad}^\varrho = H^\dagger \xi(\varrho)$ therefore

$$\bar{\mathcal{P}} \iff \min_{P \in P_g} (\min_{u \in \mathcal{U}_{ad}^\varrho} (J(u) = \|u\|^2)).$$

*Remark 3.*    Let $u \in \mathcal{U}_{ad}^\varrho$ then $u = H^\dagger \xi(\varrho)$ . Thus

$$\begin{aligned} \|u\|^2 &= \; <u,u> = <H^\dagger \xi(\varrho^i), H^\dagger \xi(\varrho_i)> \\ &= \; \|H^{-1}\xi(\varrho^i)\|^2. \end{aligned}$$

Then, we get

$$J(u) = \|H^\dagger \xi(\varrho)\|^2.$$

Let $\overline{P} \in Range(H)$,   $\overline{\varrho} = (0,0,...,b)$ with $b = \begin{pmatrix} \begin{pmatrix} 0 \\ 0 \\ 1 \end{pmatrix} \\ (0,\ldots,0) \end{pmatrix}$.

And

$$P : \quad \begin{matrix} l^2(\omega_1^N, \mathcal{X}) \\ V = (V_1, V_2, \ldots, V_N) \end{matrix} \quad \begin{matrix} \longrightarrow \\ \longrightarrow \end{matrix} \quad \begin{matrix} Range\ (H) \\ PV \end{matrix} \quad / \quad (PV)_1 = \begin{pmatrix} \begin{pmatrix} 0 \\ 0 \\ v_1^3 \end{pmatrix} \\ (0,\ldots,0) \end{pmatrix}$$

with
$(PV)_i =$

$$\begin{pmatrix} \left( 0,\ldots,0, \begin{pmatrix} 0 \\ 0 \\ v_3 \end{pmatrix} \right), \begin{pmatrix} 0 \\ cv_1^3 + (1-b)v_1^2 \\ v_1^3 \end{pmatrix}, \ldots, \begin{pmatrix} 0 \\ cv_{i-1}^3 + (1-b)v_{i-1}^2 \\ v_{i-1}^3 \end{pmatrix} \begin{pmatrix} 0 \\ cv_{i-1}^3 + (1-b)v_{i-1}^2 \\ v_1^3 \end{pmatrix} \end{pmatrix} ;$$

$$\forall i \in \omega_2^N.$$

**Theorem 1.** *For $y_i^d$, $\forall i \in \omega_1^N$, a desired output with constraint $(1-a)x_0 + x_0 y_0 + f_i = y_1^d$, optimal control allows for $\tau$-controllability, and the system's exact output controllability (E) is provided by*

$$\begin{cases} u_0 = z_1 - (1-d)z_0, \\ u_i = z_{i+1} - (1-d)z_i, & i \in \omega_1^{N-1}, \end{cases}$$

*where*

$$\begin{cases} x_i = y_i^d, \quad \forall i \in \omega_1^N, \\ y_i = \frac{(1-a)y_i^d - y_{i+1}^d + f_i}{y_i^d}, \quad \forall i \in \omega_1^{N-1}, \\ z_i = \frac{y_{i+1} - (1-b)y_i}{c}, \quad \forall i \in \omega_0^{N-2}. \end{cases}$$

*Proof.* Looking at the proof with the fixed point expression: $g(\varrho) = \varrho$, with

$$\varrho_i = \begin{pmatrix} \begin{pmatrix} x_i \\ y_i \\ z_i \end{pmatrix} \\ (\xi_{-N}, \dots, \xi_{-1}) \end{pmatrix},$$

which implies that

$$\begin{cases} x_i = \sum_{j=0}^{i-1}(1-a)^j(-x_{i-1-j}y_{i-1-j} + f_{i-1-j}) + (1-a)^i x_0, \\ y_i = cz_{i-1} + (1-b)y_{i-1}, \\ z_i \in \mathbb{R}, \quad \forall i \in \omega_1^N. \end{cases}$$

The final constraint $\tau \varrho_N = (y_1^d, \dots, y_N^d)$ implies that

$$\begin{cases} x_i = y_i^d, \quad \forall i \in \omega_1^N, \\ y_i = \frac{(1-a)y_i^d - y_{i+1}^d + f_i}{y_i^d}, \quad \forall i \in \omega_1^{N-1}, \\ z_i = \frac{y_{i+1} - (1-b)y_i}{c}, \quad \forall i \in \omega_0^{N-2}, \end{cases}$$

the optimal control enable the system (E) to have exactly output controllability indicated by $u^* = H^\dagger \xi(\varrho^{i_0})$, verify

$$\begin{cases} u_0 = z_1 - (1-d)z_0, \\ u_i = z_{i+1} - (1-d)^{i+1}z_0 - (1-d)(z_i - (1-d)^i z_0), \\ \quad = z_{i+1} - (1-d)z_i, \quad i \in \omega_1^{N-1}. \end{cases}$$

□

# 4 Numerical simulation

In this section, we conduct a numerical analysis of the system (E) to demonstrate the analytic results obtained above. This study analyzes data from non-diabetic people to assess the proposed system's ability to closely track blood glucose levels. The data used in this research was gathered from various people who do not have any history of diabetes [36]. The data, which includes daily plasma glucose and insulin profiles, is appropriate for evaluating the proposed system's ability to accurately measure blood glucose levels. The exogenous glucose injection is provided by

$$f_i = 0.3858 \times (1 + 0.33 \times \sin(3.14 \times i/72)), \quad i \in \{1, \dots, N\}.$$

The numerical findings are depicted in Figures 1–3. All simulations in this part were executed using MATLAB (R2023). The parameters and data are available in the articles [36], and [26]: $a = 0.000296$, $b = 0.045$, $c = 0.000012$, $d = 0.268$, $X = g = 6$, $Y = h = 200$, $Z = k = 0.0533$, and $N = 500$. The corresponding optimal cost is $u_i = 53.63$ and $y_d^i = 6$ $i \in \{1, \dots, N\}$.
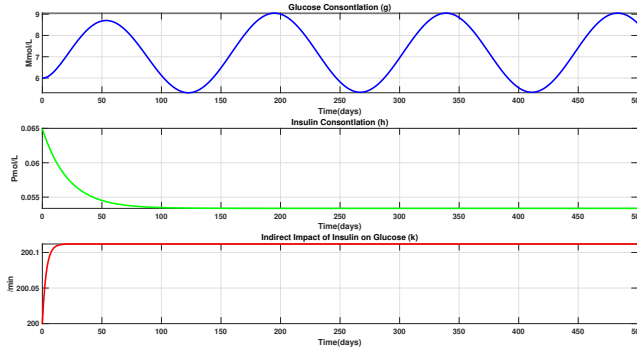
**Figure 1.** Glucose dynamics change and the effect of insulin without control.

Without any control, Figure 1 represents the dynamics of glucose and insulin concentrations in mmol/L over 500 days. The glucose concentration wave in the first graph (g) begins at roughly 6 mmol/L and rises to less than 9 mmol/L as the peak value after 50 days. Then it drops to its lowest point over the next 100 days before rising to a maximum of exactly 9 mmol/L by 200 days. Later, the wave repeats its pattern, going down and up for the entire period. The second figure (h) shows insulin concentration in picomoles per liter (pmol/L), which drops exponentially from 0.065 pmol/L to 0.055 pmol/L in 100 days until stabilizing at nearly zero pmol/L for the rest of the 400 days. The third graph (k) depicts insulin's indirect impact on glucose (/min), which increases exponentially from 200 to 200.1 in 30 days before remaining steady at 200.15 for the rest of the 470 days. This suggests that the body's insulin sensitivity is declining with time. In general, we can see from Figure 1 that glucose is influenced by insulin levels, while the effect of insulin on glucose varies over time. Furthermore, the effect of glucose is inversely proportional to insulin concentration, and it is clear that insulin concentration has a positive effect on glucose concentration.
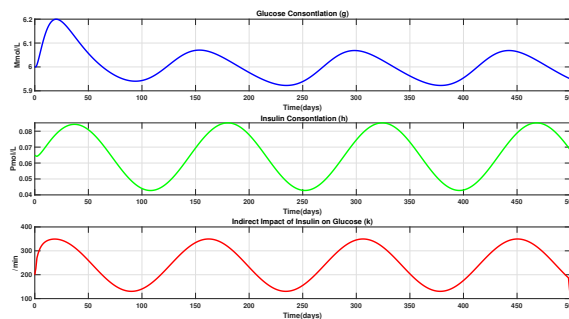


**Figure 2.** Glucose dynamics change and the effect of insulin with control.

By implementing control, Figure 2 highlights the positive impact of regulated insulin

delivery on glucose regulation over the same 500-day duration. Graph (g) clearly shows that the glucose concentration is effectively kept within a narrower range, varying between 5.94 mmol/L and 6.07 mmol/L during a period of 450 days. This represents a significant improvement over Figure 1, with glucose levels consistently within or very close to the normal fasting range. This improvement is due to the controlled sinusoidal pattern of insulin concentration, as illustrated in the second graph (h) shows insulin concentration in picomoles per liter (pmol/L), which ranges from approximately 0.04 to 0.08 pmol/L. This improvement is attributed to the controlled sinusoidal pattern of insulin concentration (h), ranging from approximately 0.04 pmol/L to 0.08 pmol/L. As shown in the third graph (k) depicts insulin's indirect impact on glucose, an increased and regulated indirect effect on glucose is the outcome of this regulated insulin administration, and it displays a distinct cyclical pattern between approximately 110 and 350. Overall, the two figures demonstrate that controlling insulin levels can be helpful in maintaining stable blood glucose levels. Figure 1 shows that when insulin is not actively regulated, glucose oscillates more significantly. While Figure 2 shows that active insulin control yields more stable glucose levels and fewer significant oscillations.
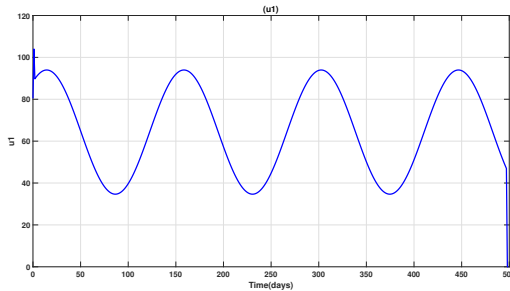


**Figure 3.** Control curve for the function $u_i$.

For the function $u_i$, which repeats its cycle at regular intervals, typically every 125 days, Figure 3 shows the periodic pattern with a maximum value of around 95 and a low value of about 35.

## 4.1 Glucose regulation models: a comparative analysis

Our work and that of Lui et al. [26] both deal with mathematical models of blood glucose levels, but they use different approaches and make different assumptions. The statistics from the American Diabetes Association (ADA) are compared in Figure 4 and Table 2. The American Diabetes Association (ADA) has established 24-hour blood glucose level recommendations for both healthy and sick individuals, measured in millimoles per milliliter. In scientific research, differential equations often represent the processing and absorption of glucose. We may learn a lot by comparing the approaches and assumptions used in these equations. This study's results were compared to those of Liu et al. [26], who investigated hyperglycemia by the manipulation of blood glucose levels. In our results, as shown in Table 3, the glucose levels are within the normal fasting range, while Table 4 shows higher levels above the normal range, indicating poor glucose control. Table 3 shows a relatively stable insulin

concentration, peaking at 90 pmol/L and returning to 80 pmol/L by the end of the 24-hour period. The insulin concentration in Table 4 is much higher, peaking at 250 pmol/L. This could mean that the body is responding strongly to insulin, which could cause low blood sugar or other problems. Table 3 demonstrates more effective and stable control of blood glucose levels, while Table 4 shows higher glucose levels, suggesting poor insulin administration and potential hyperglycemia. The proposed mathematical model, which utilizes a fixed-point theorem for control, is superior in maintaining stable glucose levels compared to Table 4. The findings emphasize the importance of controlled insulin delivery for optimal blood glucose regulation, crucial for effective diabetes management. Our novel approach, primarily based on the fixed point method, yielded quantitatively presented results indicating that the blood glucose level falls within the world health organization's reported range of 5.95 mmol/L to 6.07 mmol/L.
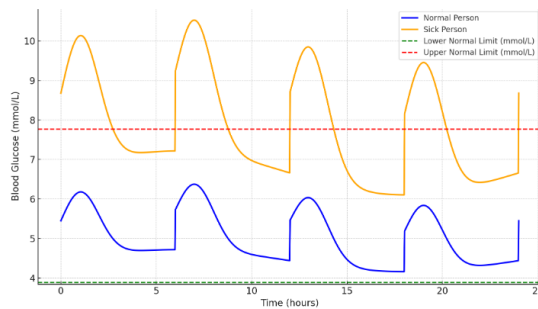


**Figure 4.** Comparison of blood Glucose Levels over one day (mmol/L) from the American Diabetes Association (ADA).

**Table 2.** Comparison of Blood Glucose Levels (mmol/L) over 24 hours from the American Diabetes Association (ADA).

| Time (hours) | Glucose (Normal, mmol/L) | Glucose (Sick, mmol/L) |
|:---:|:---:|:---:|
| 0.00 | 5.45 | 8.68 |
| 6.00 | 6.95 | 11.11 |
| 12.00 | 5.20 | 7.56 |
| 18.00 | 4.85 | 6.95 |
| 24.00 | 5.45 | 8.68 |

**Table 3.**   Concentrations of glucose (mmol/L) and insulin(pmol/L) in this research article.

| Time (h) | Glucose Concentration | Insulin Concentration |
|----------|----------------------|----------------------|
| 0 | 5.0 | 80 |
| 4 | 5.5 | 85 |
| 8 | 6.0 | 90 |
| 12 | 5.7 | 88 |
| 16 | 5.3 | 82 |
| 20 | 4.9 | 78 |
| 24 | 5.0 | 80 |

**Table 4.**  Concentrations of glucose (mmol/L) and insulin (pmol/L) over a 24-hour period, Liu et al. [26].

| Time (h) | Glucose Concentration | Insulin Concentration |
|----------|----------------------|----------------------|
| 0 | 7.0 | 100 |
| 4 | 8.0 | 150 |
| 8 | 10.0 | 200 |
| 12 | 9.0 | 250 |
| 16 | 8.5 | 200 |
| 20 | 7.5 | 150 |
| 24 | 7.0 | 100 |

## 5   Conclusions

This research successfully presented and analyzed a mathematical nonlinear discrete model of diabetes mellitus that describes the role of insulin in glucose regulation in the body. It is important to understand how to regulate insulin more effectively in the treatment of diabetes. Our goal is to regulate the levels of glucose in the blood by applying control strategies. We investigate the proposed framework for glucose and insulin dynamics both analytically and numerically. We can characterize the set of admissible controls with an appropriate mapping through an application based on the fixed point theorem. We applied the output controllability problem to a nonlinear discrete distributed system with energy constraints. The concept that we used in this study allows us to approximate the curve of statistics produced in the study to the curve of real statistics while maintaining a minimal to non-existent error rate. The results of this study and the theories we used in this work, was effective in maintaining insulin and blood glucose balance. We investigated the efficacy of the optimal control technique in tracking blood glucose using numerical simulation,

which significantly reduced blood glucose fluctuations. Our research offers helpful insights into the modeling of diabetes as well as a framework for developing treatment strategies effectively. It suggests improving care and quality of life for diabetics. Future work for this study could be opened to many topics, adding more obstacles in models, and this study can be applied to delayed models.

# References

[1] A.H. Adoum, M.S.D. Haggar, T. Djaokamla and J.M. Ntaganda. A mathematical model of glucose homeostasis in Chad context. *Journal of Ramanujan Society of Mathematics & Mathematical Sciences*, **10**(1), 2022. https://doi.org/10.56827/JRSMMS.2022.1001.13.

[2] A.H. Adoum, M.S.D. Haggar and J.M. Ntaganda. Mathematical modelling of a glucose-insulin system for type 2 diabetic patients in Chad. *Mathematical Modelling and Numerical Simulation with Applications*, **2**(4):244–251, 2022.

[3] K.I.A. Ahmed, H.D.S. Adam, M.Y. Youssif and S. Saber. Different strategies for diabetes by mathematical modeling: Applications of fractal–fractional derivatives in the sense of Atangana–Baleanu. *Results in Physics*, **52**:106892, 2023. https://doi.org/10.1016/j.rinp.2023.106892.

[4] K.I.A. Ahmed, H.D.S. Adam, M.Y. Youssif and S. Saber. Different strategies for diabetes by mathematical modeling: modified minimal model. *Alexandria Engineering Journal*, **80**:74–87, 2023. https://doi.org/10.1016/j.aej.2023.07.050.

[5] M.H. Alshehri, S. Saber and F.Z. Duraihem. Dynamical analysis of fractional-order of IVGTT glucose–insulin interaction. *International Journal of Nonlinear Sciences and Numerical Simulation*, **24**(3):1123–1140, 2023. https://doi.org/10.1515/ijnsns-2020-0201.

[6] R. Bakke. Mathematical modeling of diabetic patient model using intelligent control techniques. *Lecture notes on data engineering and communications technologies*, pp. 17–35, 2023. https://doi.org/10.1007/978-981-99-0609-3_2.

[7] B. Basturk, Z.K. Ozerson and A. Yuksel. Evaluation of the effect of macronutrients combination on blood sugar levels in healthy individuals. *Iranian journal of public health*, **50**(2):280, 2021. https://doi.org/10.18502/ijph.v50i2.5340.

[8] L. Benahmadi, M. Lhous and A. Tridane. Mathematical modeling of COVID-19 in Morocco and the impact of controlling measures. *Commun. Math. Biol. Neurosci.*, **2021**:Article–ID 53, 2021.

[9] L. Benahmadi, M. Lhous, A. Tridane and M. Rachik. Output trajectory controllability of a discrete-time sir epidemic model. *Mathematical Modelling of Natural Phenomena*, **18**:16, 2023. https://doi.org/10.1051/mmnp/2023015.

[10] R.N. Bergman, Y.Z. Ider, C.R. Bowden and C. Cobelli. Quantitative estimation of insulin sensitivity. *American Journal of Physiology-Endocrinology And Metabolism*, **236**(6):E667, 1979. https://doi.org/10.1152/ajpendo.1979.236.6.E667.

[11] R.N. Bergman, L.S. Phillips and C. Cobelli. Measurement of insulin sensitivity and $\beta$-cell glucose sensitivity from the response to intravenous glucose. *J. Clin. Invest*, **68**:1456–1467, 1981. https://doi.org/10.1172/JCI110398.

[12] R.N. Bergman, L.S. Phillips and C. Cobelli. Physiologic evaluation of factors controlling glucose tolerance in man: measurement of insulin sensitivity and beta-cell

glucose sensitivity from the response to intravenous glucose. *The Journal of clinical investigation*, **68**(6):1456–1467, 1981. https://doi.org/10.1172/JCI110398.

[13] D.N. Chalishajar, R.K. George, A.K. Nandakumaran and F.S. Acharya. Trajectory controllability of nonlinear integro-differential system. *Journal of the Franklin Institute*, **347**(7):1065–1075, 2010. https://doi.org/10.1016/j.jfranklin.2010.03.014.

[14] J.J. Chamberlain, A.S. Rhinehart, C.F. Shaefer and A. Neuman. Diagnosis and management of diabetes: synopsis of the 2016 American Diabetes Association standards of medical care in diabetes. *Annals of internal medicine*, **164**(8):542–552, 2016. https://doi.org/10.7326/M15-3016.

[15] M. Chan. WHO global report on diabetes. *World Health Organization*, 2016.

[16] N.H. Cho, J.E. Shaw, S. Karuranga, Y. Huang, J.D. da Rocha Fernandes, A.W. Ohlrogge and B. Malanda. IDF diabetes atlas: Global estimates of diabetes prevalence for 2017 and projections for 2045. *Diabetes research and clinical practice*, **138**:271–281, 2018. https://doi.org/10.1016/j.diabres.2018.02.023.

[17] A. Cinar and K. Turksoy. Modeling glucose and insulin concentration dynamics. *Advances in Artificial Pancreas Systems: Adaptive and Multivariable Predictive Control*, pp. 33–50, 2018. https://doi.org/10.1007/978-3-319-72245-0_4.

[18] B. Farahmand, M. Dehghani, N. Vafamand, A. Mirzaee, R. Boostani and J.K. Pieper. Robust nonlinear control of blood glucose in diabetic patients subject to model uncertainties. *ISA transactions*, **133**:353–368, 2023. https://doi.org/10.1016/j.isatra.2022.07.009.

[19] M. Farman, A. Ahmad, A. Zehra, K.S. Nisar, E. Hincal and A. Akgul. Analysis and controllability of diabetes model for experimental data by using fractional operator. *Mathematics and Computers in Simulation*, **218**:133–148, 2024. https://doi.org/10.1016/j.matcom.2023.11.017.

[20] M. Farman, A. Hasan, C. Xu, K.S. Nisar and E. Hincal. Computational techniques to monitoring fractional order type-1 diabetes mellitus model for feedback design of artificial pancreas. *Computer Methods and Programs in Biomedicine*, **257**:108420, 2024. https://doi.org/10.1016/j.cmpb.2024.108420.

[21] M. Farman, M.U. Saleem, M.O. Ahmed and A. Ahmad. Stability analysis and control of the glucose insulin glucagon system in humans. *Chinese Journal of Physics*, **56**(4):1362–1369, 2018. https://doi.org/10.1016/j.cjph.2018.03.037.

[22] M. Gallenberger, W. Castell, B.A. Hense and C. Kuttler. Dynamics of glucose and insulin concentration connected to the b-cell cycle: model development and analysis. *Theoretical Biology and Medical Modelling*, **9**:1–22, 2012. https://doi.org/10.1186/1742-4682-9-46.

[23] R. Hovorka, V. Canonico, L.J. Chassin, U. Haueter, M. Massi-Benedetti, M.O. Federici, T.R. Pieber, H.C. Schaller, L. Schaupp and T. Vering. Nonlinear model predictive control of glucose concentration in subjects with type 1 diabetes. *Physiological measurement*, **25**(4):905, 2004. https://doi.org/10.1088/0967-3334/25/4/010.

[24] D. Infante. Trailblazing discoveries: The top 5 diabetes research breakthroughs of 2023. *News-Medical Life science*, 2023.

[25] M. Lhous, M. Rachik, J. Bouyaghroumni and A. Tridane. On the output controllability of a class of discrete nonlinear distributed systems: a fixed point theorem approach. *International Journal of Dynamics and Control*, **6**:768–777, 2018. https://doi.org/10.1007/s40435-017-0315-9.

[26] W. Liu. A mathematical model for the robust blood glucose tracking. *Mathematical Biosciences and Engineering*, **16**(2):759–781, 2019. https://doi.org/10.3934/mbe.2019036.

[27] R. Luft. Oskar Minkowski: discovery of the pancreatic origin of diabetes, 1889. *Diabetologia*, **32**(7):399–401, 1989. https://doi.org/10.1007/BF00271257.

[28] K. Lunze, T. Singh, M. Walter, M.D. Brendel and S. Leonhardt. Blood glucose control algorithms for type 1 diabetic patients: A methodological review. *Biomedical signal processing and control*, **8**(2):107–119, 2013. https://doi.org/10.1016/j.bspc.2012.09.003.

[29] D.J. Magliano and E.J. Boyko. Diabetes around the world in 2021. *International Diabetes Federation*, 2021.

[30] C.D. Man, R.A. Rizza and C. Cobelli. Meal simulation model of the glucose-insulin system. *IEEE Transactions on biomedical engineering*, **54**(10):1740–1749, 2007. https://doi.org/10.1109/TBME.2007.893506.

[31] S.M. Pappada, B.D. Cameron and P.M. Rosman. Development of a neural network for prediction of glucose concentration in type 1 diabetes patients. *Journal of diabetes science and technology*, **2**(5):792–801, 2008. https://doi.org/10.1177/193229680800200507.

[32] S. Saber and A. Alalyani. Stability analysis and numerical simulations of IVGTT glucose-insulin interaction models with two time delays. *Mathematical Modelling and Analysis*, **27**(3):383–407, 2022. https://doi.org/10.3846/mma.2022.14007.

[33] A. Sharma, H. Singh and R. Nilam. A methodical survey of mathematical model-based control techniques based on open and closed loop control approach for diabetes management. *International Journal of Biomathematics*, **15**(07), 2022. https://doi.org/10.1142/s1793524522500516.

[34] H. Shi, Y. Ge, H. Wang, Y. Zhang, W. Teng and L. Tian. Fasting blood glucose and risk of stroke: A dose–response meta-analysis. *Clinical nutrition*, **40**(5):3296–3304, 2021. https://doi.org/10.1016/j.clnu.2020.10.054.

[35] J. Sturis, K.S. Polonsky, E. Mosekilde and E. Van Cauter. Computer model for mechanisms underlying ultradian oscillations of insulin and glucose. *American Journal of Physiology-Endocrinology And Metabolism*, **260**(5):E801–E809, 1991. https://doi.org/10.1152/ajpendo.1991.260.5.E801.

[36] J. Sturis, E. Van Cauter, J.D. Blackman and K.S. Polonsky. Entrainment of pulsatile insulin secretion by oscillatory glucose infusion. *The Journal of clinical investigation*, **87**(2):439–445, 1991. https://doi.org/10.1172/JCI115015.

[37] L. Tie and K.-Y. Cai. On near-controllability of nonlinear control systems. In *Proceedings of the 30th Chinese Control Conference*, pp. 131–136. IEEE, 2011.